

# Influence of Transverse Magnetic Field on Microchannel Heat Sink Performance

K. Narrein<sup>1</sup>, S. Sivasankaran<sup>2,†</sup> and P. Ganesan<sup>1</sup>

<sup>1</sup> Department of Mechanical Engineering, University of Malaya, 50603 Kuala Lumpur, Malaysia

<sup>2</sup> Institute of Mathematical Sciences, University of Malaya, 50603 Kuala Lumpur, Malaysia

†Corresponding Author Email: [sd.siva@yahoo.com](mailto:sd.siva@yahoo.com)

(Received July 18, 2015; accepted July 4, 2016)

## ABSTRACT

The aim of the present numerical investigation is to analyze the effects of transverse magnetic field on heat transfer and fluid flow characteristics in a rectangular microchannel heat sink (MCHS). The effects of Hartmann number, channel aspect ratio, total channel height and total channel width on heat transfer and fluid flow characteristics are widely investigated. The governing equations for three-dimensional steady, laminar flow and conjugate heat transfer of a microchannel are solved using the finite volume method. The obtained results are discussed with various combinations of pertinent parameters involved in the study. The results reveal that magnetic field can enhance the thermal performance of the MCHS but it is accompanied with a slight increase in pressure drop.

**Keywords:** Microchannel heat sink; Magnetic field; Pressure drop; Aspect ratio; Heat transfer.

## NOMENCLATURE

|       |                           |          |                         |
|-------|---------------------------|----------|-------------------------|
| $B_o$ | magnetic field strength   | $Re$     | Reynolds number         |
| $C_p$ | heat Capacity             | $T$      | temperature,            |
| $D$   | channel depth             | $V$      | velocity                |
| $D_h$ | hydraulic diameter        | $W$      | total Channel width     |
| $f$   | friction factor           | $W_{ch}$ | channel; width          |
| $h$   | heat transfer coefficient |          |                         |
| $Ha$  | Hartmann number           | $\alpha$ | channel aspect ratio    |
| $k$   | thermal conductivity      | $\sigma$ | electrical conductivity |
| $L$   | channel length            | $\rho$   | density                 |
| $Nu$  | Nusselt number            | $\mu$    | viscosity               |

## 1. INTRODUCTION

The demand for smaller electronic chips with higher power consumption has paved the way for various research activities to provide more efficient cooling. Cooling is required to maintain the chips at optimum temperature and to prevent it from burning. Heat transfer enhancement in micro-scale is a challenging problem and is an active area of research due to many applications. The novel idea of dispelling heat using microchannel heat sink (MCHS) was first presented by Tuckerman and Pease (1981). The MCHS was fabricated using silicon to attain a higher heat transfer rate, which is a direct implication of a lower thermal resistance. Deionized water was used as the working fluid in that study and a power density of

790 W/cm<sup>2</sup> was achieved, which eventually resulted in the substrate temperature rise of 71°C above the inlet water temperature. As a continuation to their previous work, Tuckerman and Pease (1982) further discussed challenges associated to microchannel cooling such as headering, coolant selection etc. Coolant figures of merit (CFOM) were proposed to optimize the heat transfer coefficient for either a given coolant pressure or constant pumping power.

Numerous studies by several researches (Peiyi and Little 1983; Morini 2004; Narrein *et al.* 2015a, Narrein *et al.* 2015b, Narrein *et al.* 2016, Sivasankaran and Narrein 2016) have helped in the development of new ideas and understanding in the field of heat transfer, computational fluid dynamics

(CFD) and MCHS. Kim and Mudawar (2010) developed detailed analytical heat diffusion models for a number of channel geometries of microchannel heat sink such as rectangular, inverse-trapezoidal, trapezoidal, triangular and diamond shaped cross-sections. The analytical results agree fairly with two-dimensional numerical results for a range of Biot numbers. Fedorov and Viskanta (2000) numerically investigated the three-dimensional incompressible laminar conjugate heat transfer in a microchannel heat sink that used for electronic packaging applications. The model was validated with the existing thermal resistance and friction factor data. The temperature/heat flux distribution and the average heat transfer characteristics were presented in detail. They also found that the Poiseuille flow assumption was not always accurate and careful assessment was needed to evaluate its validity to ensure minimal errors in predicting friction coefficients.

Lee *et al.* (2005) conducted an experimental investigation to validate the accordance of classical correlations on conventional sized channels in order to predict the thermal characteristics of a single-phase flow through rectangular microchannels. The range of the microchannel width considered was from 194 to 534  $\mu\text{m}$  where the channel depth was set to be five times of the width for each respective case. Deionized water was allowed to flow in a parallel configuration through ten rows of channel. The microchannel was made out of copper. The authors concluded that the previous numerical predictions are close with experimental results. The thermal behavior in microchannel can be estimated using conventional analysis given that the boundary conditions are exactly matched as per that used in the experiment.

Tsai and Chein (2007) performed an analytical study to analyze the performance of nanofluid-cooled microchannel heat sinks. Copper-water and carbon nanotube-water nanofluids were used as the working fluid. The channel where fluid flows was modeled as porous media to obtain the velocity and temperature distribution. The researchers found that nanofluid was able to reduce the temperature difference between the MCHS bottom wall and bulk nanofluid, thus reducing the conductive thermal resistance. Significant increment in the thermal resistance was observed due to the higher viscosity of nanofluids as compared to other coolants. Thermal enhancement was also observed when nanofluid was used for MCHS which has an optimum porosity and aspect ratio. However, such enhancement did not persist for higher porosity and aspect ratios. Pfahler *et al.* (1989, 1990) experimentally investigated the laminar fluid flow through a trapezoidal MCHS using various types of fluid. The Poiseuille number ( $fRe$ ) increased with increasing Reynolds number; however it was generally lower than the predicted value.

Peng and Peterson (1996) conducted a numerical investigation on single-phase forced convective heat transfer in rectangular MCHS using water as the working fluid. It was concluded from the results that the geometry was an important factor in determining

the heat transfer and fluid flow characteristics through a MCHS. Empirical correlations were proposed for the Nusselt number and friction factor. Rahman and Gui (1993, 1998) experimentally investigated forced convection of water through a trapezoidal MCHS. It was found that the Nusselt number in laminar flow was much higher as compared to that of turbulent flow and no extreme change was observed in the transition region. In addition, the data obtained for friction factor is appeared indecisive.

Moraveji *et al.* (2013) numerically investigated the cooling performance and pressure drop in a mini-channel heat sink using nanofluids. Two different nanoparticles with various volume concentration and velocities were investigated. It was found that the heat transfer coefficient increased with increasing nanoparticle concentration and Reynolds number. Fani *et al.* (2013) presented the effect of nanoparticle size on thermal performance of nanofluid in a trapezoidal microchannel heat sink. CuO-Water nanofluid with 100-200nm and 1-4% concentration were considered. A significant increase in pressure drop was observed as the concentration was increased. Heat transfer decreased with the increase of particle size.

Liu *et al.* (2013) conducted an experimental study to analyze the effect of non-uniform heating in the performance of microchannel heat sinks. Two types of manifold were used for the investigation. One that has a side inlet entrance, which is normal to the direction of the main flow and the other, which is parallel to the flow direction. In the case of uniform heating, the latter manifold showed better results due to better flow distribution. Better performance was also observed when the heater was positioned at the inlet for non-uniform heating. In a separate study, Hung and Yan (2013) numerically investigated the effects of tapered-channel on thermal performance of microchannel heat sink. The researchers concluded that thermal resistance and the width-tapered ratio is not monotonic at constant pumping power. A similar result was observed for the height-tapered ratio case as well.

Sohel *et al.* (2013) presented the results for the heat transfer performance and thermos-physical properties of nanofluids in circular microchannel.  $\text{Al}_2\text{O}_3$ ,  $\text{TiO}_2$ , and CuO water based nanofluid were used in their analysis. The researchers concluded that CuO-Water based nanofluid showed better heat transfer enhancement compared to  $\text{Al}_2\text{O}_3$  and  $\text{TiO}_2$  nanofluid. Mansoor *et al.* (2012) investigated the fluid flow and heat transfer in a rectangular microchannel under high heat flux condition. Water was used as the cooling fluid and the microchannel substrate considered was copper. An increase in heat transfer coefficient was observed with increasing heat flux. The authors proposed a correlation to predict the average Nusselt number for microchannels with simultaneously developing flow. Cito *et al.* (2012) numerically investigated the mass transfer rated in capillary-driven flow in microchannels. Wall mass transfer rate enhancement was observed due to recirculation. The authors presented correlations for Sherwood number and

Reynolds number, contact angle and time.

Magneto-convection is a convective flow of an electrically conducting fluid in the presence of the imposed magnetic field. Numerous studies by several researches have helped in the development and understanding of fluid flow and heat transfer characteristics in the presence of magnetic field (Bhuvanewari *et al.* (2011), Malleswaran and Sivasankaran (2016), Sivasankaran *et al.* (2011a), Sivasankaran and Bhuvanewari (2011), Sivasankaran *et al.* (2011b), Karthikeyan *et al.* (2016)). Magneto-convection in an enclosure is numerically investigated by Sivasankaran *et al.* (2011c) and Malleswaran *et al.* (2013). Aminossadati *et al.* (2011) numerically investigated the laminar forced convection through a horizontal microchannel under the influence of a transverse magnetic field in the middle section. Al<sub>2</sub>O<sub>3</sub>-water based nanofluid was used as the working fluid and the microchannel was partially heated in the mid-section. Effects of Reynolds number, nanoparticle volume fraction and Hartmann number were investigated. Results from their study portray an increased heat transfer at higher Reynolds and Hartmann number. However, no efforts were made to study the effects of pressure drop. Furthermore, a two-dimensional study was conducted by the researches; hence the results may not be the same for actual three-dimensional problems as the additional wall effects may play a vital role in determining the exact heat transfer enhancement due to additional pressure drop. Numerous other studies have also helped in the understanding and advancement in the field of MCHS (Niazmand *et al.*, 2010, Ramiar *et al.*, 2012, Zade *et al.*, 2015, Wang *et al.*, 2015, Hamed *et al.*, 2016, Kaya, 2016).

To the author's best knowledge, limited attempts are made to study in detail the effects of transverse magnetic field on three-dimensional laminar heat transfer and fluid flow characteristics in a microchannel heat sink; hence, this has motivated the present study. Electrical components have the potential to produce magnetic fields and this wasted energy can be used to further enhance the heat transfer through the MCHS. Previous studies did not tackle the effects that have been investigated in the present study. The current study examines the three-dimensional laminar flow with the effects of different Hartmann number (0-25), channel aspect ratio (1-3), channel height (300-350 μm) and its total channel width (250-300 μm) extensively. Results of interests such as Nusselt number and pressure drop is reported to illustrate the effects of transverse magnetic field on these parameters.

## 2. MATHEMATICAL MODEL

### 2.1 Governing Equations

The microchannel heat sink considered in this study is shown schematically in Figure 1. The heat is transferred from the bottom wall of the MCHS to the working fluid which is water in this case. Several assumptions are made on the operating conditions of the MCHS: (i) the MCHS operates under steady-

state conditions; (ii) the fluid remains single phase along the MCHS; (iii) the properties of the MCHS material are temperature independent; (iv) the external heat transfer effects are ignored; (v) the outer walls of the MCHS are adiabatic. Three-dimensional incompressible laminar flow is considered for the entire study.

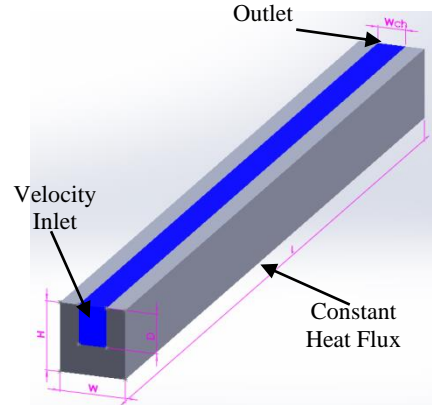


**Fig. 1. Schematic diagram of the computational domain of MCHS.**

The governing equations for flow and heat transfer in the MCHS are (Xia *et al.* 2011):

Continuity equation:

$$\nabla \cdot \vec{v} = 0 \quad (1)$$

Momentum equation:

$$(\vec{v} \cdot \nabla) \vec{v} = \frac{1}{\rho} \nabla p + \nu \Delta \vec{v} + \frac{1}{\rho} (j \times B) \quad (2)$$

Energy equation:

$$(\vec{v} \cdot \nabla) T = \alpha \Delta T \quad (3)$$

The water is set to flow through the channel and the bottom wall of the MCHS is heated with a constant heat flux of  $1 \times 10^6$  W/m<sup>2</sup>. The inlet velocity is varied to produce the Reynolds number in the range of Re = 500-1000. The inlet temperature of the water is set to 300K. The outlet is set to pressure outlet and the wall between the channel (fluid region) and solid region is set to "coupled for heat transfer". The outer wall of the MCHS is set as adiabatic.

The Nusselt number is calculated using the following equation:

$$Nu = \frac{h D_h}{k} \quad (4)$$

where  $h$  is the heat transfer coefficient,  $D_h$  is the hydraulic diameter and  $k$  is the thermal conductivity of the working fluid. The heat transfer coefficient is calculated based on the following equation:

$$h = \frac{q}{\Delta T} \quad (5)$$

where  $q$  is the heat flux of the intermediate wall between the solid and fluid.  $\Delta T$  represented by the temperature difference between the intermediate

wall and the average bulk fluid temperature.

### 2.2 Grid Independence Test

A grid independence test is performed to evaluate the effects of grid sizes on the results. Four sets of mesh are generated using hexagonal elements with 7262 nodes, 0.29 million nodes, 0.68 million nodes and 1.77 million nodes, respectively. Laminar flow is considered for this test where the inlet temperature of the channel is set to 300 K with a velocity of 4 m/s. The bottom wall is heated with a constant heat flux of  $1 \times 10^6$  W/m<sup>2</sup>. The error for each model is computed in relation to the 1.77 million nodes model. As shown in Table 1, the 1.77 million and 0.68 million nodes grid produce almost identical results along the MCHS with an error of 0.09%. Hence, a domain with approximately 0.5 to 0.6 million nodes is chosen for all cases to reduce computing time. The summary of the grid independence test is shown in Table 1.

**Table 1 Grid Independence Test Results**

| Nodes     | Outlet Temperature (K) | Percentage Error (%) |
|-----------|------------------------|----------------------|
| 7 262     | 319.779                | 2.18                 |
| 292 317   | 313.897                | 0.30                 |
| 684 632   | 313.222                | 0.09                 |
| 1 773 648 | 312.943                | -                    |

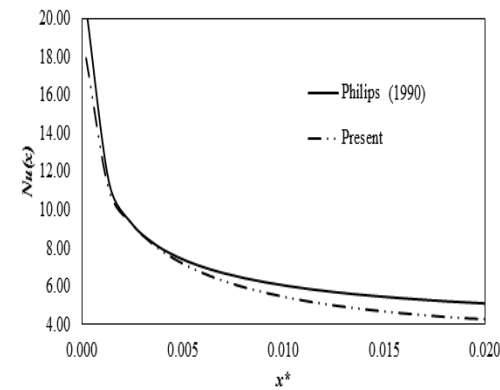
### 2.3 Model Validation

The code validation is done based on the geometry which was first used by Xia *et al.* (2011). Water with an inlet velocity of 4 m/s was set to flow through the channel and the bottom wall of the MCHS is heated with a constant heat flux of  $1 \times 10^6$  W/m<sup>2</sup>. The thermal field results are compared with the analytical results suggested by Philips (1990). It can be seen from Fig. 2a that the thermal field results are in good agreement. In addition, the flow field and magnetic field results are also validated with the correlation presented by Steinke & Kandlikar (2006) and Back (1968) which is in good agreement as depicted in Fig. 2b and Fig. 2c.

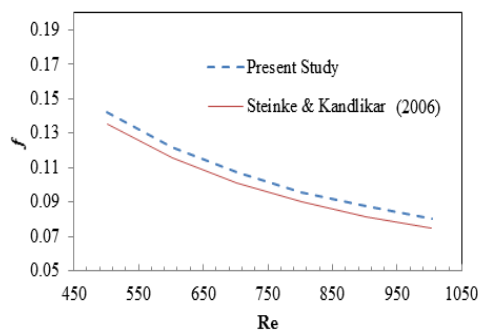
### 2.4 Numerical Procedure

The numerical computations are carried out by solving the governing equations along with the boundary conditions using the finite volume method. The SIMPLE algorithm is adopted to investigate the flow field. The second-order upwind differencing scheme is used for the convective terms. The diffusion term in the momentum and energy equations are approximated by the second-order central difference scheme which gives a stable solution. Numerical simulation is carried out for different combinations of pertinent parameters such as (i) Hartmann number, (ii) channel aspect ratio, (iii) total channel height and (iv) total channel width to investigate the effects on MCHS. The convergence criterion is set to be  $1 \times 10^{-5}$ . Second order discretization scheme is used for pressure, momentum and energy equations. The under-

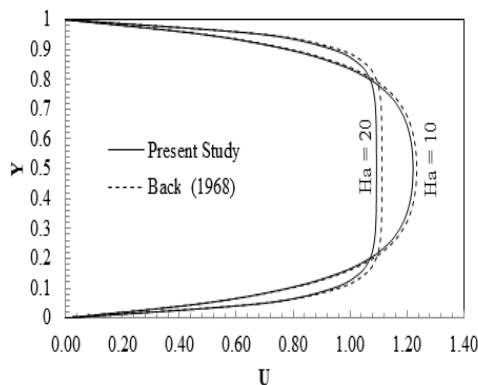
relaxation factor parameters for pressure and momentum is set to 0.3 and 0.7 respectively.



(a)



(b)



(c)

**Fig. 2. Comparison of the present results of the (a) thermal field, (b) flow field and (c) magnetic field across the MCHS with the results of previous analytical studies.**

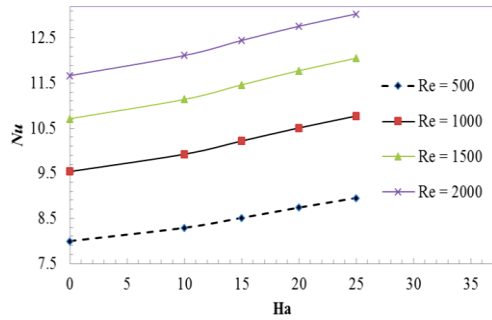
## 3. RESULTS AND DISCUSSION

The effects of transverse magnetic field on the thermal and flow fields of the MCHS are analyzed and discussed in this section. For the first case, the effects of Hartmann number is investigated for  $Ha = 0, 10, 15, 20$  and  $25$ . In the second case, the aspect ratio is investigated where  $\alpha = 1, 1.5, 2, 2.5$  and  $3$ . The aspect ratio is defined by the channel depth divided by the channel width. In the subsequent cases the total channel height and total channel width

is investigated. All the cases are investigated in the range of  $Re = 500-2000$ .

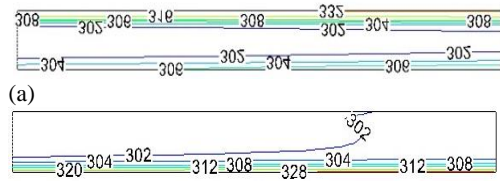
### 3.1 Effects of Transverse Magnetic Field on the Thermal Field

The effect of Hartmann number on the thermal field is presented via the Nusselt number as shown in Fig. 3.



**Fig. 3. Variation of Nusselt number with Hartmann number for various Reynolds number.**

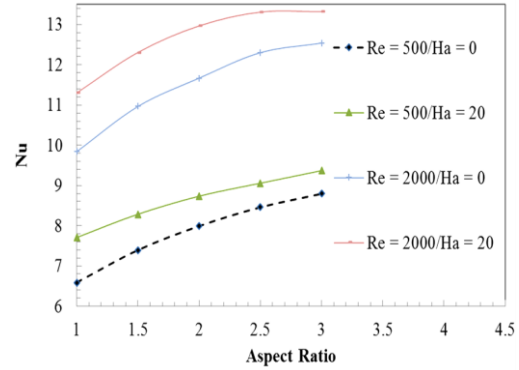
It can be seen from the figure that the Nusselt number increases on increasing the Reynolds and Hartmann numbers. In normal cases, the flow becomes fully developed after a certain entry length. However, the magnetic field introduced in this study prevents the fluid from reaching a fully developed state which directly leads to the enhancement in heat transfer. An undeveloped flow would tend to have smaller thermal boundary layer thicknesses which ensure larger temperature gradient between the hot surface and fluid. This will directly lead to a convective heat transfer enhancement because of the larger heat transfer rate. As the magnitude of the magnetic field is increased, the effect is further intensified to produce better heat transfer enhancement. This effect can be further presented by comparing the temperature contour at the tube near end region which is illustrated in Fig. 4.



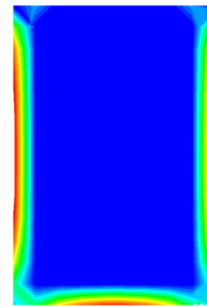
**Fig. 4. Temperature Contour for (a)  $Ha = 0$  and (b)  $Ha = 25$  for  $Re = 500$ .**

The effect of variation of the aspect ratio of MCHS performance is portrayed in Fig.5. Increase in the aspect ratio leads to an increase in the Nusselt number and the increment is further enhanced with the presence of the magnetic field for the same reason which is described earlier. The aspect ratio is varied by increasing the channel depth,  $D$  (i.e. height) while keeping the constant channel width. Previous literatures suggest that local heat transfer conductance vary around the edge of the channel and move towards zero at the square corners (Kays and

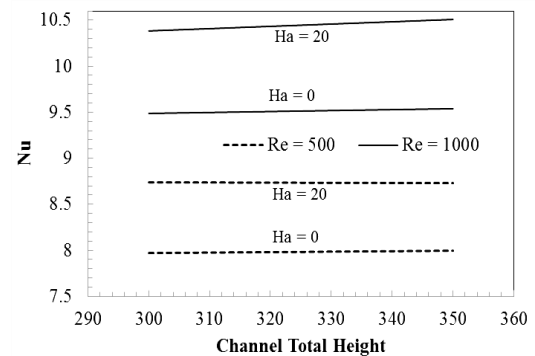
Crawford, 1993). Svino and Siegel (1964) found that poor convection occurs due to lower velocities at the corners. The dominance of these effects on convective heat transfer tends to fade off at higher aspect ratio which is also observed in this study where the Nusselt number increases with increasing the aspect ratio. The surface heat flux contour for this study is shown in Fig.6.



**Fig. 5. Variation of Nusselt number with Aspect Ratio for various Nusselt number.**



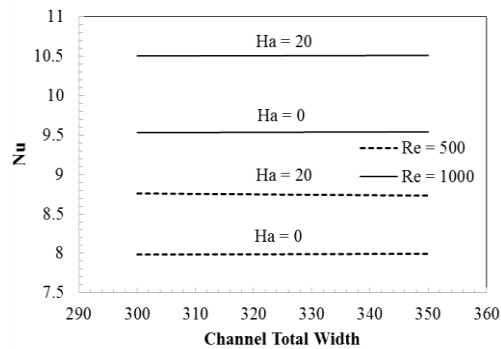
**Fig. 6. Surface heat flux contour for channel with 1.5 aspect ratio.**



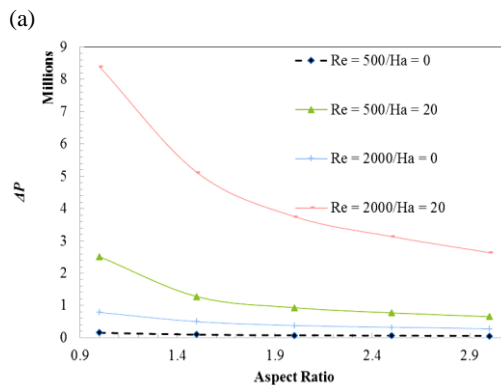
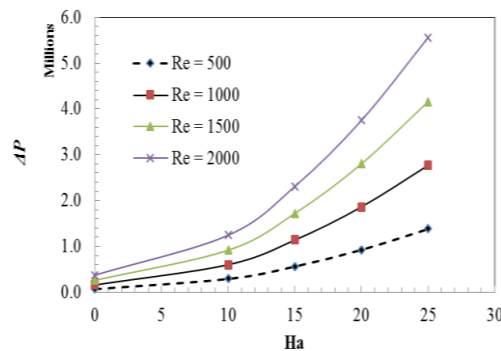
**Fig. 7. Variation of Nusselt number with total channel height.**

Fig.7. shows the variation of Nusselt number with total channel height ( $H$ ). A minor change in Nusselt number is observed when the channel height is increased from 300 to 350  $\mu\text{m}$ . The thickness between the channel and bottom surface plays a vital role in determining the total thermal resistance. An optimum thickness is required for optimum heat transfer which is studied and presented in detail by Biswal *et al.* (2009). The effect of channel total width ( $W$ ) is presented in Fig.8. A considerable change in

Nusselt number is also observed and this can be accounted for the larger surface area. Since the heat flux is set to constant, a larger surface area leads to a larger magnitude of total heat transfer.



**Fig. 8. Variation of Nusselt number with total channel width.**



**Fig. 9. Pressure drop for various Reynolds number for (a) different Hartmann number, (b) different aspect ratio.**

### 3.1 Effects of Transverse Magnetic Field on the Flow Field

The flow field performance of the MCHS is evaluated in terms of pressure drop. The value is obtained by acquiring the net area-weighted average difference between the inlet and outlet.

Fig.9a. shows the pressure drop for different values of the Hartmann number. It can be seen that the pressure drop increases with increasing the Hartmann number. The effect of magnetic field

prevents the flow from reaching a fully developed state to a certain extent. While this is happening, the velocity at wall tends to be higher than that of a fully developed flow which directly leads to a higher shear stress at this region. A higher wall shear stress would eventually lead to a higher pressure drop. In the case of different aspect ratios, it is observed from Fig.9b that pressure drop tends to decrease with increasing the aspect ratio.

A larger hydraulic diameter allows for a relatively lower velocity which results in a much lower shear stress at the near wall region. This can help to reduce the overall pressure drop through the MCHS. The effect of total channel height and width on the pressure drop (not illustrated here) showed no major difference. However, a small variation is present and this can be accounted for the variance in density due to some changes in the overall fluid temperature which can have a direct effect on the velocity.

## 5. CONCLUSIONS

Thermal and flow field characteristics of a MCHS under the influence of magnetic field are studied numerically. The effects of Hartmann number, aspect ratio, total channel height and total channel width on flow and temperature field are investigated.

- Magnetic field is able to increase the convective heat transfer substantially. It is found that convective heat transfer can be enhanced by increasing the magnitude of the magnetic field but is accompanied by significant amount of pressure drop.
- Nusselt number seems to also increase with increasing the aspect ratio with a reduction in pressure drop.
- Considerable changes in the thermal and flow fields are also observed when the total channel height and width is varied.

## REFERENCE

Aminossadati, S. M., A. Raisi and B. Ghasemi, (2011). Effects of magnetic field on nanofluid forced convection in partially heated microchannel. *International Journal of Non-Linear Mechanics* 46(10), 1373-1382.

Back, L. H. (1968). Laminar heat transfer in electrically conducting fluids flowing in parallel plate channels. *International Journal of Heat and Mass Transfer* 11(11), 1621-1636.

Bhuvanewari, M., S. Sivasankaran and Y. J. Kim (2011). Magneto-convection in an Enclosure with Sinusoidal Temperature Distributions on Both Side Walls. *Numerical Heat Transfer Part A* 59, 167-184.

Biswal, L., S. Chakraborty and A. Som (2009). Design and Optimization of single-phase liquid cooled microchannel heat sink. *IEEE Trans. Compon. Package Technology* 32(4), 876-886.

- Cito, S., J. Pallares, A. Fabregat and I. Katakis (2012). Numerical simulation of wall mass transfer rates in capillary-driven flow in microchannels. *International Communication of Heat and Mass Transfer* 39, 1066-1072.
- Fani, B., A. Abbassi and M. Kalteh (2013). Effect of nanoparticles size on thermal performance of nanofluid in a trapezoidal microchannel-heat-sink. *International Journal of Heat and Mass Transfer* 45, 155-161.
- Fedorov, A. G., and R. Viskanta (2000). Three-dimensional conjugate heat transfer in the microchannel heat sink for electronic packaging. *International Journal of Heat and Mass Transfer* 43(3), 399-415.
- Hamed, A., M. Shamsiri, M. Charmiyan, and E. Shirani (2016). Investigation of nonlinear electrokinetic and rheological behaviors of typical non-Newtonian biofluids through annular microchannels. *Journal of Applied Fluid Mechanics* 9(1), 367-378.
- Hung, T. C. and W. M. Yan (2013). Effects of tapered-channel design on thermal performance of microchannel heat sink. *International Communication of Heat and Mass Transfer* 39(9), 1342-1347.
- Karthikeyan, S., M. Bhuvaneshwari, S. Sivasankaran and S. Rajan (2016). Soret and Dufour effects on MHD mixed convection heat and mass transfer of a stagnation point flow towards a vertical plate in a porous medium with chemical reaction, radiation and heat generation. *Journal of Applied Fluid Mechanics* 9(3), 1447-1455.
- Kaya, F. (2016). Numerical investigation of effects of ramification length and angle on pressure drop and heat transfer in a ramified microchannel. *Journal of Applied Fluid Mechanics* 9(2), 767-772.
- Kays, W. M., and M. E. Crawford (1993). *Convective Heat and Mass Transfer*, 3rd ed, McGraw-Hill, USA.
- Kim, S. M., and I. Mudawar (2010). Analytical heat diffusion models for different micro-channel heat sink cross-sectional geometries. *International Journal of Heat and Mass Transfer* 53(19-20), 4002-4016.
- Lee, P. S., S. V. Garimella and D. Liu (2005). Investigation of heat transfer in rectangular microchannels. *International Journal of Heat and Mass Transfer* 48(9), 1688-1704.
- Liu, C. K., S. J. Yang, Y. L. Chao, K. Y. Liou and C. C. Wang (2013). Effect of non-uniform heating on the performance of the microchannel heat sinks. *International Communication of Heat and Mass Transfer* 43, 57-62.
- Malleswaran, A., and S. Sivasankaran (2016). Numerical Simulation on MHD Mixed Convection in a Lid-driven Cavity with Corner Heaters. *Journal of Applied Fluid Mechanics* 9(1), 311-319.
- Malleswaran, A., S. Sivasankaran and M. Bhuvaneshwari (2013). Effect of heating location and size on MHD convection in a lid-driven cavity. *International Journal of Numerical Methods for Heat and Fluid Flow* 23(5), 867-884.
- Mansoor, M. M., K. C. Wong and M. F. M. Siddique (2012). Numerical investigation of fluid flow and heat transfer under high heat flux using rectangular micro-channels. *International Communication of Heat and Mass Transfer* 39(2), 291-297.
- Moraveji, M. K., R. M. Ardehali and A. Ijam (2013). CFD investigation of nanofluid effects (cooling performance and pressure drop) in mini-channel heat sink. *International Communication of Heat and Mass Transfer* 40, 58-66.
- Morini, G. L. (2004). Single-Phase convective heat transfer in microchannels: a review of experimental results. *International Journal of Thermal Sciences* 43(7), 631-651.
- Narrein, K., S. Sivasankaran and P. Ganesan (2016). Numerical investigation of two-phase laminar pulsating nanofluid flow in helical microchannel. *Numerical Heat Transfer Part A* 69(8), 921-930.
- Narrein, K., S. Sivasankaran and P. Ganesan (2015a). Convective Heat transfer and fluid flow analysis in a helical microchannel filled with a porous medium. *Journal of Porous Media* 18(8), 1-10.
- Narrein, K., S. Sivasankaran and P. Ganesan (2015b). Two-Phase Analysis of Helical Microchannel Heat Sink using Nanofluids. *Numerical Heat Transfer Part A* 68, 1-14.
- Niazmand, H., A. A. Jaghargh and M. Renksizbulut (2010). Slip-flow and heat transfer in isoflux rectangular microchannels with thermal creep effects. *Journal of Applied Fluid Mechanics* 3(2), 33-41.
- Peiyi, W. and W. A. Little (1983). Measurement of friction factors for the flow of gases in very fine channels used for microminiature Joule-Thomson refrigerators. *Cryogenics* 23(5), 273-277.
- Peng, X. F. and G. P. Peterson (1996). Convective heat transfer and flow friction for water flow in microchannel structures. *International Journal of Heat and Mass Transfer* 39(12), 2599-2608.
- Pfahler, J., J. Harley, H. Bau and J. Zemel (1989). Liquid transport in micron and submicron channels. *Sensors and Actuators A: Physical* 22(1-3), 431-434.
- Pfahler, J., J. Harley, H. Bau and J. Zemel (1990). Liquid and gas transport in small channels. In *Proceedings of ASME WAM Micro Structures, Sensors and Actuators, DSC* 19, 149-157.
- Phillips, R. J. (1990). *Advances in thermal modeling of electronic components and systems*,

- Hemisphere Publishing Corporation, New York, USA 10-25.
- Rahman, M. M. and F. Gui (1993). Experimental measurements of fluid flow and heat transfer in microchannel cooling passages in a chip substrate. *Advances in Electronic Packaging, ASME EEP* 4(2), 685-692.
- Rahman, M. M. and F. Gui (1998). Design, fabrication, and testing of microchannel heat sinks for aircraft avionics cooling. In *Proceedings of the 28<sup>th</sup> Intersociety Energy Conversion Engineering Conference* 1-6.
- Ramiar, A., A. A. Ranjbar and S. H. Hosseinizadeh (2012). Effect of axial conduction and variable properties on two-dimensional conjugate heat transfer of AL<sub>2</sub>O<sub>3</sub>-EG/water mixture nanofluid in microchannel. *Journal of Applied Fluid Mechanics* 5(3), 79-87.
- Sivasankaran, S., A. Malleswaran, J. Lee and P. Sundar (2011a). Hydro-magnetic combined convection in a lid-driven cavity with sinusoidal boundary conditions on both sidewalls. *International Journal of Heat and Mass Transfer* 54, 512-525.
- Sivasankaran, S. and K. Narrein (2016). Numerical investigation of two-phase laminar pulsating nanofluid flow in helical microchannel filled with a porous medium. *International Communications in Heat and Mass Transfer* 75, 86-91.
- Sivasankaran, S. and M. Bhuvanewari (2011). Effect of thermally active zones and direction of magnetic field on hydro-magnetic convection in an enclosure. *Thermal Science* 15(S2), S367-S382.
- Sivasankaran, S., J. Lee and M. Bhuvanewari (2011c). Effect of a partition on hydro-magnetic convection in a partitioned enclosure. *Arabian Journal of Science and Engineering* 36(7), 1393-1406.
- Sivasankaran, S., M. Bhuvanewari, Y. J. Kim, C. J. Ho and K. L. Pan (2011b). Magneto-convection of cold water near its density maximum in an open cavity with variable fluid properties. *International Journal of Heat and Fluid Flow* 32, 932-942.
- Sohel, M. R., R. Saidur, M. F. M. Sabri, M. Kamalisatvestani, M. M. Elias and A. Ijam (2013). Investigating the heat transfer performance and thermophysical properties of nanofluids in a circular micro-channel. *International Communication of Heat and Mass Transfer* 42, 75-81.
- Steinke, M. E. and S. G. Kandlikar (2006). Single-phase liquid friction factors in microchannels. *International Journal of Thermal Sciences* 45, 1073-1083.
- Svino, J. M. and R. Siegel (1964). Laminar forced convection in rectangular channels with unequal heat addition on adjacent sides. *International Journal of Heat and Mass Transfer* 7(7), 733-741.
- Tsai, T. H. and R. Chein (2007). Performance analysis of nanofluid-cooled microchannel heat sinks. *International Journal of Heat and Fluid Flow* 28(5), 1013-1026.
- Tuckerman, D. B. and R. F. W. Pease (1981). High-performance heat sinking for VLSI. *Electron Device Letters, IEEE* 2(5), 126-129.
- Tuckerman, D. B. and R. F. W. Pease (1982). Ultrahigh Thermal Conductance Microstructures for Cooling Integrated Circuits. *32nd Electronic Components Conference, IEEE CH 781-4*, 145-149.
- Wang, S., M. Zhao, X. Li and S. Wei (2015). Analytical solutions of time periodic electroosmotic in a semicircular microchannel. *Journal of Applied Fluid Mechanics* 8(2), 323-327.
- Xia, G., L. Chai, H. Wang, M. Zhou and Z. Cui (2011). Optimum thermal design of microchannel heat sink with triangular reentrant cavities. *Applied Thermal Engineering* 31(6-7), 1208-1219.
- Zade, A. A., M. Renksizbulut and J. Friedman (2015). Ammonia Decomposition for Hydrogen Production in Catalytic Microchannels with Slip/Jump Effects. *Journal of Applied Fluid Mechanics* 8(4), 703-712.